Figure S1, related to Figure 1

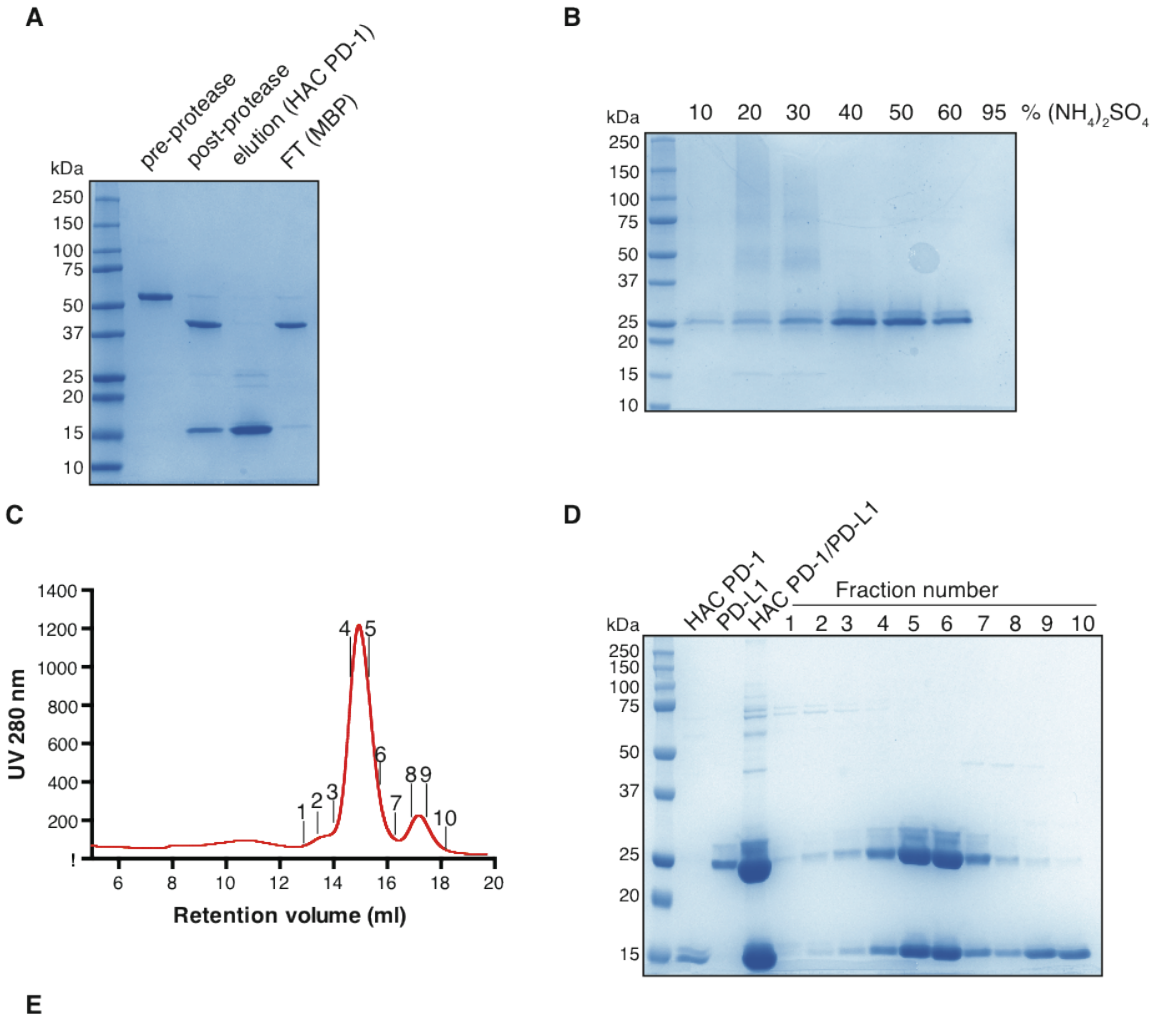

E

aa position	wt PD-1	HAC PD-1
64	V	H
65	L	V
66	N	V
68	Y	H
70	M	E
74	N	G
78	K	T
122	L	V
125	A	V
132	A	I

Figure S1, related to Figure 1. Purification of HAC PD-1 and PD-L1 complex

(A and B) HAC PD-1 and PD-L1 expression and purification were verified by coomassie gel staining. (C) Size exclusion chromatography of the complex formed by HAC PD-1 and PD-L1 and (D) coomassie gel staining of the corresponding fractions relative to the peaks in (C). (E) Table representing the position of each mutated aminoacid of HAC PD-1 and the corresponding residue in wild-type PD-1. Pink column shading indicates core mutations, while the remaining residues directly contact PD-L1.

Figure S2, related to Figure 1

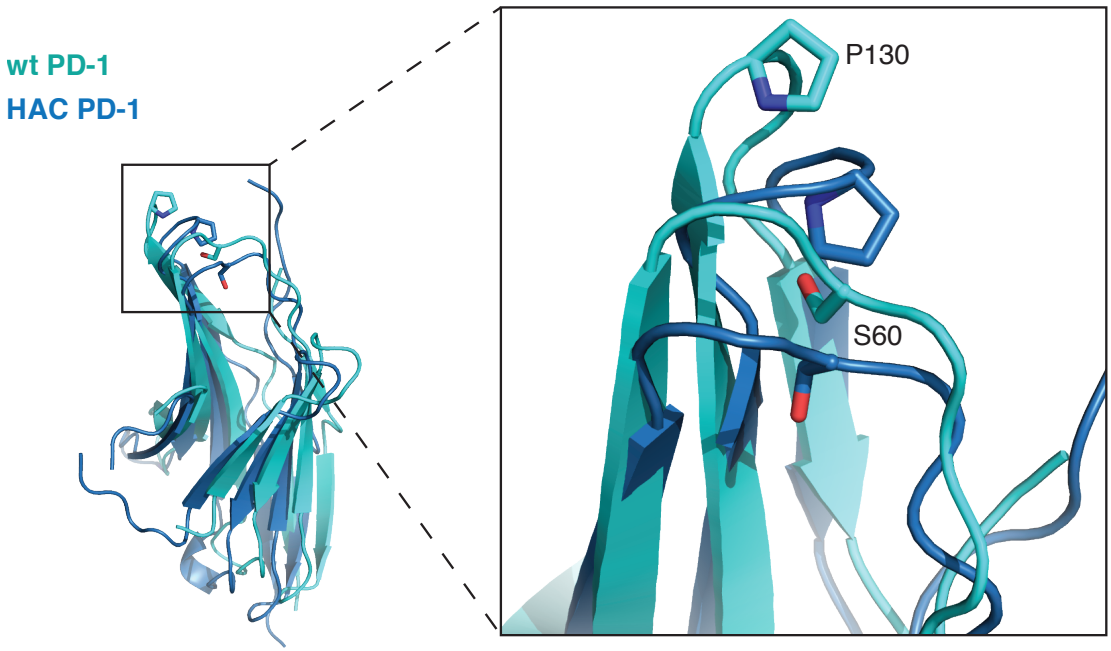

Figure S2, related to Figure 1. Superimposition wild-type PD-1 and HAC PD-1.
Wild type PD-1 and HAC PD-1 are depicted in cyan and blue respectively. Superimposition of HAC PD-1 with wild-type PD-1 shows significant conformational rearrangement in the loops containing Ser60 and Pro130.

Figure S3, related to Figure 2

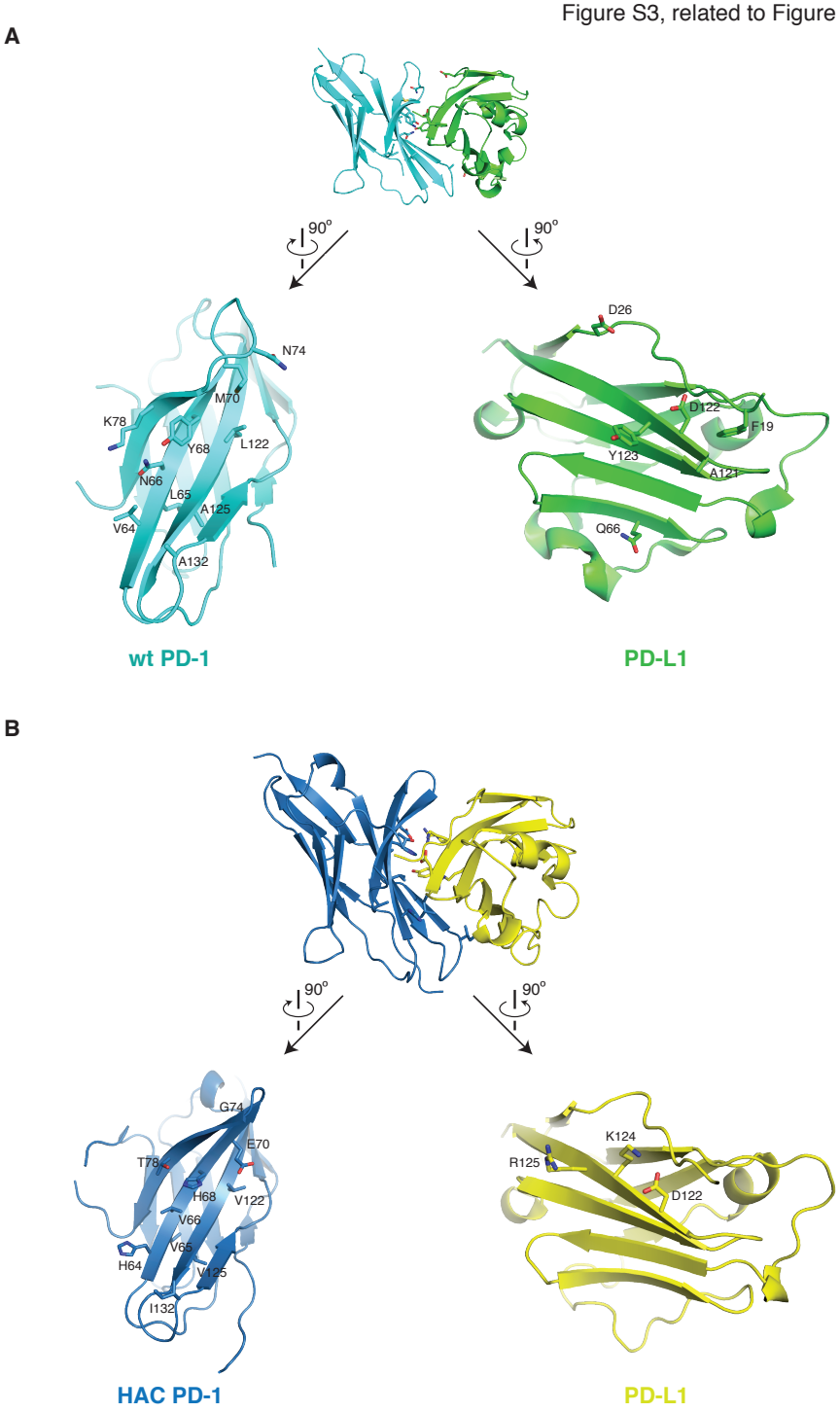

Figure S3, related to Figure 2. HAC PD-1 mutations are located at the interface with PD-L1. Open book presentation of wild type PD-1/PD-L1 and HAC PD-1/PD-L1 complex (A) Top panel shows the side view of the complex between wild-type PD-1 and PD-L1; bottom panel displays either side of the interface. Residues mutagenized in HAC PD-1 are shown as sticks, as are residues in PD-L1 that directly interact with these amino acids. (B) Top panel shows thge side view of the complex between HAC PD-1 and PD-L1; bottom panle displays either side of the interface. Residues mutagenized in HAC PD-1 are shown as sticks, as are residues in PD-L1 that directly interact with these amino acids.

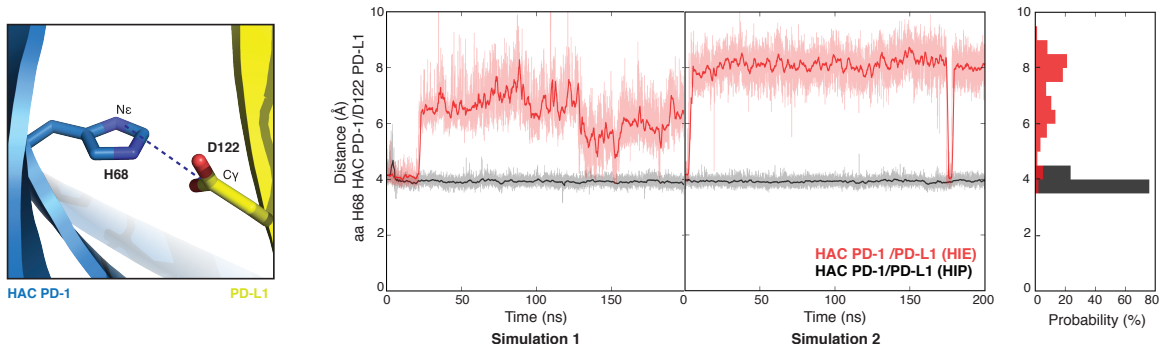

Figure S4, related to Figure 5. Electrostatic interactions between H68 on HAC PD-1 and D122 on PD-L1 may facilitate the binding of the two proteins. (A) Temporal evolution of distances between the side chains of residue 68 on PD-1 and the Cγ of D122 on PD-L1. For HAC PD-1/PD-L1 (HIE) and HAC PD-1/PD-L1 (HIP), Nε on H68 (PD-1) and the C γon D122 (PD-L1) were used to calculate the distances. HIE refers to His68 in unprotonated state, while HIP refers to His68 in a protonated state.

Table S1, related to Figure 1

Data collection *	
Number of crystals	1
Space group	$P4_1$
Cell dimensions	
a, b, c (Å)	86.9, 86.9, 111.8
α, β, γ (°)	90, 90, 90
Resolution (Å)	50 – 2.9 (3.08 – 2.90)
$CC_{1/2}$	99.7 (27.3)
<I/σI>	8.37 (0.55)
Completeness (%)	99.8 (99.8)
Multiplicity	6.1 (5.8)
Refinement	
Resolution (Å)	47.03 – 2.90 (2.96 – 2.90)
No. reflections	18559 (1359)
R_{work}/R_{free} (%)	20.75 / 25.96
No. atoms	
Protein	5080
Solvent	34
B-factors (Å^2)	
HAC PD-1	117.2
PD-L1	118.8
Solvent	89.9
RMS deviations	
Bond angles (°)	0.568
Bond lengths (Å)	0.003
Ramachandran	
Favored (%)	96.7
Allowed (%)	3.3
Outliers (%)	0

* Highest shell values in parenthesis

Table S1, related to Figure 1. Data collection and refinement statistics.

System	His68	PD-1 residues	PD-L1 residues	Time scale (ns)	Box volume (Å^3)	Protein length (Å)[a]	Image distance (Å)[b]
HAC PD-1/PD-L1	HIP	33 - 146	18 - 132	2*200	4.53E+5	61.63	86.23
wt PD-1/PD-L1	-	33 - 146	18 - 132	2*200	4.29E+5	62.38	84.65
HAC PD-1	HIP	33 - 146		2*500	2.87E+5	41.56	74.05
wt PD-1	-	33 - 146		2*500	2.79E+5	44.40	73.38
HAC PD-1/PD-L1	HIE	33 - 146	18 - 132	2*200	4.53E+5	61.63	86.23

Table S2, related to Figure 4. System used for the simulations. In each case the simulations were performed at least in duplicates. a. The length of the protein is the longest edge needed to put the protein into a cubic box. b. The image distance is the distance between two images of a system in the periodic boundary condition.